



## Surface plasmon polariton in metal-insulator-metal configuration

Rida Ahmed Ammar and Mostefa Lemerini

*Theoretical Physics Laboratory, Faculty of Sciences, Physics Department, University of Tlemcen, Tlemcen, Algeria*

Received 28 Dec 2015; Revised 24 Jul 2016; Accepted 2 Aug 2016

### Abstract

The optics of the surface plasmon resonance has been known for a long time. In the configuration multilayer, the optical coupling of a wave incident to collective oscillations of electrons along an interface between a metal and a dielectric is governed by the thickness of metal and gap layers. The surface plasmon excitations excited by an electromagnetic wave in the visible band ( $\lambda = 633$  nm). For the metal, in particular a frequency on their dielectric permittivity dependence and described by the Drude-Lorentz model and using the effective-index approach and an explicit expression for the propagation constant of gap surface plasmon polaritons (G-SPPs) obtained for moderate gap widths.

**Keywords:** Drude-Lorentz, surface Plasmon polariton, wave propagation, optical waveguides.

### 1. Introduction

Surface plasmon polaritons (SPP) are electromagnetic excitations propagating at the interface between a dielectric and a conductor (usually metal) material possessing opposite signs of the real part of their dielectric permittivities, evanescently confined in the perpendicular direction. These electromagnetic surface waves arise via the coupling of the electromagnetic fields to oscillations of the conductor's electron plasma. Taking the wave equation as a starting point, this section describes the fundamentals of surface plasmon polaritons both in metal /dielectric multilayer structures (IMI and semi-infinite MIM waveguides) [1, 2].

The TM polarized SP mode is uniquely characterized by its magnetic field lying in the plane of the metal-insulator surface and perpendicular to the wave propagation direction. The metal commonly used to excite surface plasmon polaritons (SPPs) is silver (Ag) due to their remarkable optical properties described by the frequency dependent complex permittivity  $\epsilon_m(\omega) = \epsilon_m^r(\omega) + i\epsilon_m^i(\omega)$  in the Drude-Lorentz model ( $\epsilon_m^r < 0$ ,  $|\epsilon_m^r| \gg \epsilon_m^i$ ). Since the SPR is the resonance phenomenon corresponding to an energetic transfer from incident light to SPPs.

The E7 [3, 4], nematic liquid crystals mixture contains cyanobiphenyl and cyanoterphenol components, at a specific composition, which possess relatively high birefringence and positive dielectric anisotropy. Due to these properties, it is widely used in polymer dispersed liquid crystals [5]. The specific composition is critical to ensure physical

\* ) For Correspondence. E-mail: [a\\_reda130@live.fr](mailto:a_reda130@live.fr), [rammar31@yahoo.com](mailto:rammar31@yahoo.com)

properties and characteristic of the liquid crystal. The specific composition is critical to ensure physical properties and characteristic of the liquid crystal. Even small changes can have pronounced effects on factors such as the nematic to isotropic transition, and glass transition temperatures. E7 is used as the dielectric  $\epsilon_d$  in the temperature 25 °C on MIM configuration. We wish to clarify that we are working under conditions of plasmon wave excite the surface polariton by an electromagnetic wave in the act of taking the negative real part of the dielectric permittivity of the metal. The characteristic parameters of the guide are the depth of propagation of electromagnetic waves in the metal medium, the permittivity of the metal and the middle of the opening, the dimensions (length and width) of the guide, the relationship of the dispersion depends mainly the effective index, and the cutoff frequency. In this work, we developed a geometry of the waveguides for confining propagating resonant modes. The main feature of the dimensions is the wavelength sub-length scale with respect to the wavelength  $\lambda$  of the excitation wave. In their simplest form, the light guides consist of layered material media. For that light energy can be propagated and confined through the guide, the indices of these media are recorded by optical usual conditions [19, 20].

## 2. The Drude-Lorentz model:

Drude-Lorentz model is often used for parameterization of the optical constants of metals. In addition to the conduction electrons, the Drude-Lorentz model takes into account the bound electrons. The interband transition of electrons from filled bands to the conduction band can significantly influence the optical response. In alkali metals, these transitions occur at high frequencies and provide only small corrections to the dielectric function in the optical domain. These metals are well described by the Drude model. On the other side, in noble metals a correction must be made to the dielectric function. It is due to transitions between the bands d and the conduction band s-p. The contribution of bound electrons to the dielectric function can be described by the Lorentz model. To the above Drude dielectric function, a Lorentzian term is added [23]:

$$\epsilon_{DL}(\omega) = \epsilon_D(\omega) + \epsilon_L(\omega) \quad (1)$$

Vial et al. [13] suggested a single oscillator leading to a single Lorentzian additional term to well describe the permittivity of gold in the optical range compared with the classical Drude model. In this case, the relative dielectric function is [6]:

$$\epsilon_{DL}(\omega) = 1 - \frac{f_0 \omega_p^2}{\omega^2 - i \omega \Gamma_0} + \sum_{j=1}^k \frac{f_j \omega_p^2}{\Omega_j^2 - \omega^2 + i \omega \Gamma_j} \quad (2)$$

where  $\omega_p$  is the plasma frequency,  $k$  is the number of oscillators with frequency  $\Omega_j$ , strength  $f_j$ , and life time  $1/\Gamma_j$ .

Table.1: Optimized parameters of the Drude–Lorentz model for Silver metal. [4],  $\omega_p$ ,  $\Omega_j$  and  $\Gamma_j$  are in electron volts,  $f_j$  has no units.

$\omega_p = 9.01$	$f_2 = 0.124$	$f_4 = 0.840$
$f_0 = 0.845$	$\Gamma_2 = 0.452$	$\Gamma_4 = 0.916$
$\Gamma_0 = 0.048$	$\Omega_2 = 4.481$	$\Omega_4 = 9.083$
$f_1 = 0.065$	$f_3 = 0.011$	$f_5 = 5.646$
$\Gamma_1 = 3.886$	$\Gamma_3 = 0.065$	$\Gamma_5 = 2.419$
$\Omega_1 = 0.816$	$\Omega_3 = 8.185$	$\Omega_5 = 20.29$

In Fig. 1, we have plotted the real and imaginary parts of the dielectric function of silver as tabulated in [6], as well as the description achieved using the DL model. The metal has a negative real component of the permittivity in the visible and infrared wavelengths but at shorter wavelengths  $\epsilon_r$  becomes positive.

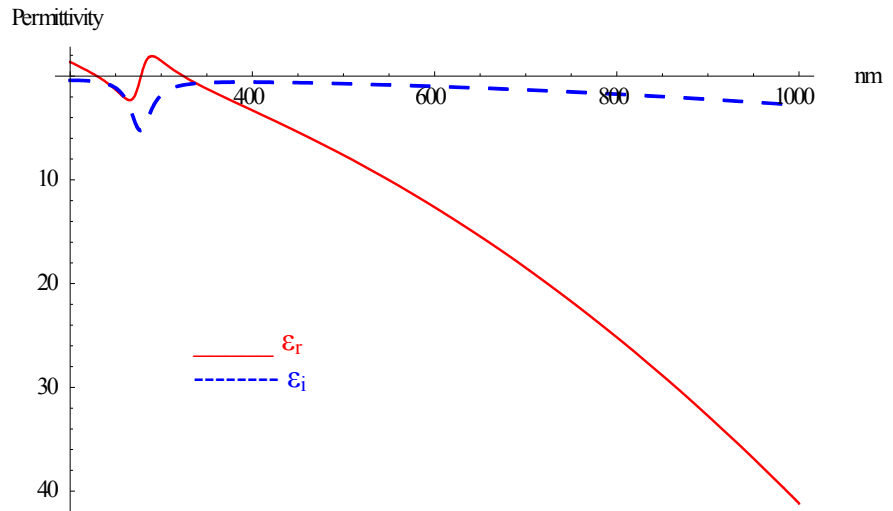


Fig.1: The real and imaginary components of the permittivity of Ag

### 3. Surface plasmons in MIM-Structure (Metal Gap):

An important extension of the simple metal surface is a three layer system, sometimes also called heterostructure [7], where each of the layers has an infinite extension in two dimensions. Two basic heterostructures can be distinguished, a dielectric gap in a metal, or MIM (metal-insulator-metal) system and a metal film surrounded by two dielectrics, or IMI (insulator-metal-insulator) system [8, 9]. Dionne and colleagues [14] extended the investigation to SP's propagation in a Ag-SiO<sub>2</sub>-Ag plasmonic (slot) waveguide and determined dispersion relation, energy density and localization for the symmetric and anti-symmetric gap plasmons with respect to the middle plane. One advantage of a MIM-structure is the strong confinement of the field in the dielectric, which is due to a small penetration depth ( $\sim 20$  nm) into the metal on each side of the gap. For the same structure, the propagation lengths of 10  $\mu\text{m}$  are supported with localization of the field in the gap of  $\sim 20$  nm. Dionne et al. [14, 15] also pointed out the additional benefit of those structures for simultaneous use with conventional electronic devices. We consider the gap is the E7 nematic liquid crystal.

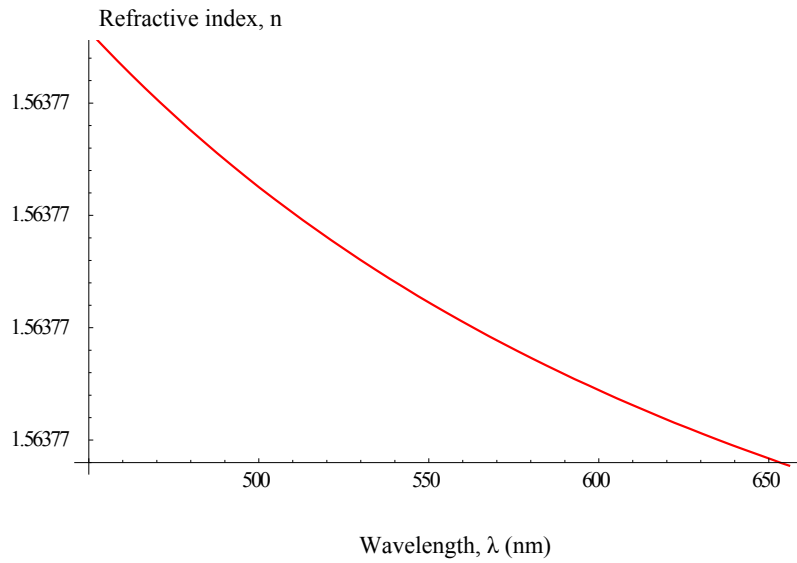


Fig. 2: The refractive index of the liquid crystal (E7) as a function of wavelength between 450-656 nm [3].

Fig. 2 shows the refractive index of E7 as a function of wavelength between 400 and 650 nm, which refractive index decrease with the increasing of wavelength. We consider the dielectric is the E7 nematic liquid crystal at  $T=25\text{ }^{\circ}\text{C}$ . The complex dielectric function  $\epsilon_d$  and the complex index of refraction  $\hat{n}$  are defined as [10]:

$$\epsilon_d = \epsilon_1 + i \epsilon_2 = \hat{n}^2 = (n + i k)^2 \tag{3}$$

At  $T=25\text{ }^{\circ}\text{C}$  and  $\lambda=633\text{ nm}$ , we have  $n_e=1.7305$ ,  $n_o=1.5189$ , [3]

where :  $\hat{n} = n + i 0 = n = \frac{n_e+2 n_o}{3} = 1.58943$  and  $\epsilon_d = \epsilon_1 = n^2 = 2.5263$ .

In this section we consider two infinite metal planes separated by a gap filled with a E7 nematic liquid crystal in which a film plasmon propagates constitute a MIM [16, 17, 18, 19, 20, 21, 22] (metal-insulator-metal) or simply a slot waveguide. We consider the SPP modes in the symmetric MIM configuration of a thin dielectric layer with the thickness  $w$  being sandwiched between two metal surfaces. When two identical SPP modes start overlapping with each other for small layer thicknesses, the dispersion relation for the metal gap of the symmetric field distribution can be written as [1, 11].

$$\tanh(k_z^{(d)} \frac{w}{2}) = -\frac{\epsilon_d k_z^{(m)}}{\epsilon_m k_z^{(d)}} \text{ and } k_z^{(m,d)} = \sqrt{\beta^2 - \epsilon_{(m,d)} k_0^2} \tag{4}$$

where  $\beta$  denotes the propagation constant of the fundamental gap surface plasmons polariton (GSPP) mode with the transverse field component  $E_z$ , having the same sign across the gap, and  $\epsilon_{m,d}$  are the permittivities of metal and insulator (E7). For sufficiently small gap widths ( $w \rightarrow 0$ ), one can use the approximation  $\tanh(x) \approx x$  resulting in the following expression [1, 11]:

$$\beta \approx k_0 \sqrt{\epsilon_d + 0.5 \left(\frac{\alpha}{k_0}\right)^2 + \sqrt{\left(\frac{\alpha}{k_0}\right)^2 \left(\epsilon_d - \epsilon_m + 0.25 \left(\frac{\alpha}{k_0}\right)^2\right)}} \quad (5)$$

with  $\alpha = -\frac{2\epsilon_d}{w\epsilon_m}$  and  $k_0 = \frac{2\pi}{\lambda}$ . Here,  $k_0$  is the wave vector of incident light,  $\lambda$  is the wavelength,  $\alpha$  represents the GSPP propagation constant in the limit of very narrow gaps ( $w \rightarrow 0$ ). The imaginary part of the propagation constant is associated with the attenuation and propagation length of the surface plasmon in the direction of propagation. The propagation constant is related to the effective index  $n_{\text{eff}}$ , propagation length  $L$  and attenuation  $b$  [2, 12] as:

$$n_{\text{eff}} = \frac{\text{Re}(\beta)}{k_0}, L = \frac{1}{2 \text{Im}(\beta)} \text{ and } b = \frac{0.2}{\ln(10)} \text{Im}(\beta) \quad (6)$$

where  $\text{Re}\{\}$  and  $\text{Im}\{\}$  denote the real and imaginary parts of a complex number, respectively; the attenuation  $b$  is in  $\text{dBcm}^{-1}$  if  $\beta$  is given in  $\text{m}^{-1}$ .

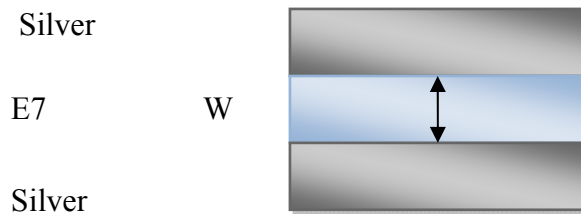
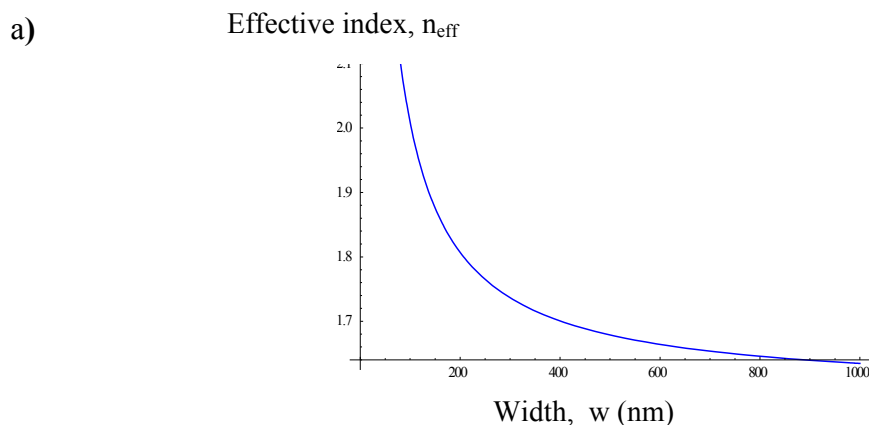


Fig. 3: Schematic of MIM plasmonic waveguide.

The schematic structure of the Ag–E7–Ag plasmonic waveguide (PW) is shown in Fig. 3. This waveguide consists of a low-index E7 stripe ( $n_{\text{E7}} = 1.58943$ ) sandwiched between a rectangular silver film ( $\lambda = 633 \text{ nm}$ ,  $\epsilon_{\text{Ag}} = -14.4688 - i 1.09378$ [6].) The E7 stripe has dimensions of  $W \text{ nm}$  width. The thickness of the silver film is taken as  $150 \text{ nm}$  largely to ensure that there are no effects of the silver film thickness on the plasmonic mode inside the E7 stripe. Coupling between the cavity resonator and input waveguide depends on the thickness of the metallic gap between the sketched pieces of Ag metal.

#### 4. Results and discussion



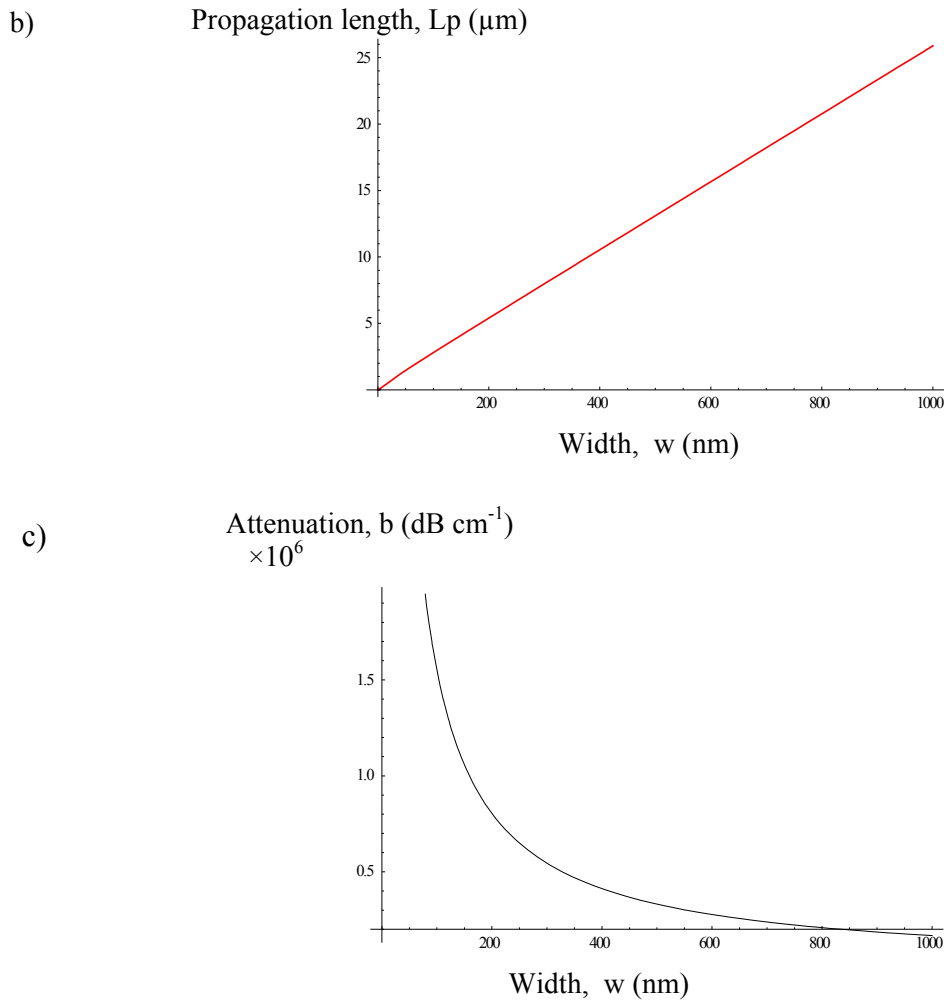


Fig.4: The effective index  $n_{\text{eff}}$ , propagation length  $L_p$ , and the attenuation  $b$ , as functions of width of the gap of the E7  $w$  for  $\lambda=633$  nm (MIM plasmonic waveguides Ag/E7/Ag,  $\epsilon_d = 2.5363$  and silver metal  $\epsilon_{\text{Ag}} = -14.4688 - i 1.09378$ .)

Fig. 4 shows the mode effective index  $n_{\text{eff}}$ , the propagation length  $L_p$  and the attenuation  $b$  of SPP mode as functions of the thickness  $w$  of the E7 stripe, where the width  $w$  of the E7 was chosen as 633 nm. The effective index, propagation length and attenuation could be acquired by numerically solving Eq. (4). We observed that increasing the width of the E7 stripe reduces the mode effective index and the attenuation, and increases the propagation length. However, for E7 thinner than 400 nm, the fundamental mode turns progressively into a plasmonic wave that propagates along the interface ( $n_{\text{eff}}=1.61$ ), leading to poor vertical confinement.

The SPP dispersion curves for Ag-E7-Ag MIM structures with various E7 layer thicknesses are illustrated in Fig. 5, calculated with the OptiFDTD [24]. The result shows decreasing in film thickness and the MIM symmetric mode exhibits a cut-off for core films.

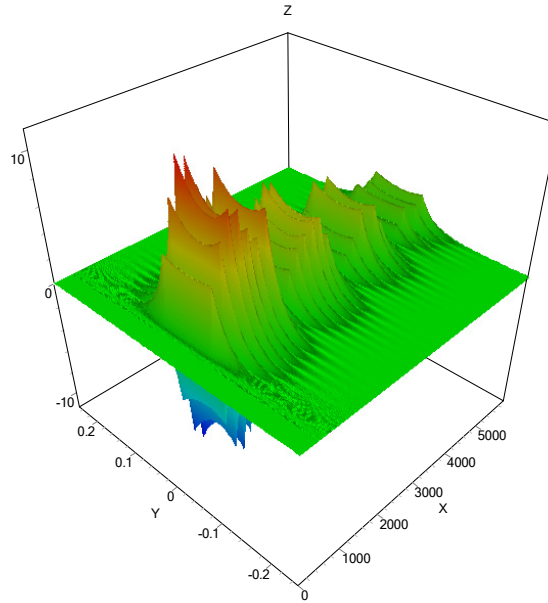


Fig.5: Geometry and characteristic tangential magnetic field profile  $H_y$  for the semi-infinite MIM wave guide core insulator thickness  $w$ , propagate along the positive  $Z$  direction.

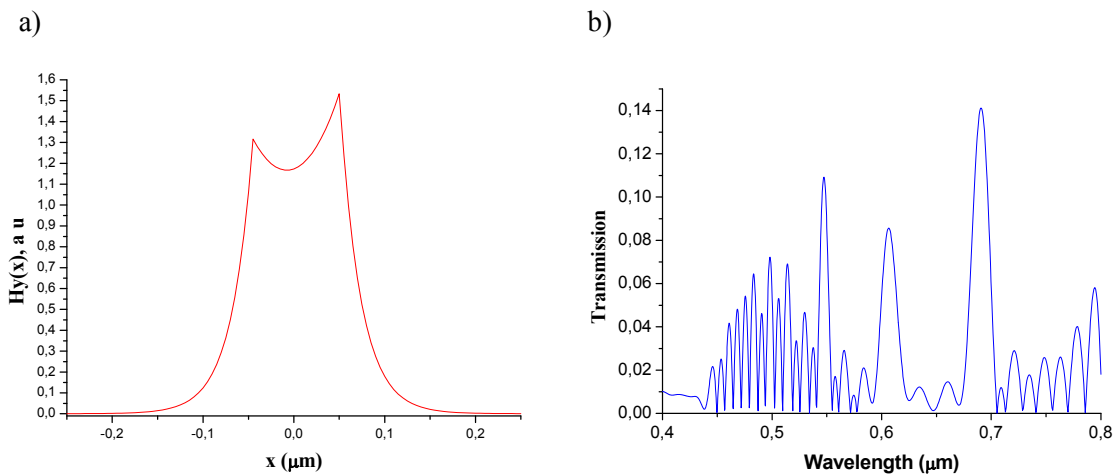


Fig.6: (a) Surface plasmon magnetic field profile of silver-E7-silver guide ( $\lambda=633\text{nm}$ ,  $2w=0.1\ \mu\text{m}$ ), and (b) the transmission spectrum.

In Fig. 6 (a), the magnetic field profile is presented in the plane  $(x, z)$  for  $\lambda=633\ \text{nm}$  (in vacuum) and for a symmetric MIM configuration with permittivities  $\epsilon_d = 2.5363$  and  $\epsilon_{Ag} = -14.4688 - i 1.09378$ . Thus, the transverse magnetic field  $H_y(x)$ , which is continuous at the interface, the gap plasmons can be excited in phase, hence the magnetic field component  $H_y$  is symmetric with respect to the centre of the gap. As the operation wavelength increases, the delocalization of the two peaks of the SPP mode in the two metal-dielectric interfaces causes more power be concentrated in the E7-core of the gap waveguide. Fig. 6(b) shows the transmission as a function of the wavelength, calculated with the OptiFDTD [24] method for the optimized gap distance of  $50\ \text{nm}$  and length  $l = 100$ . It is observed that the maximum of the transmission is  $0.7\ \mu\text{m}$ .

## 5. Conclusion

The optics of the surface plasmon resonance has been known for so long. In this paper, we discuss the use of a metal-insulator-metal (MIM) structure to generate plasmon surface polaritons. In the first step, we study the influence of the gap thickness on the resonance SPP. In the second step, we present the analytical results of the effective index, attenuation and propagation length as a function of wavelength for disposal, which are excited by an electromagnetic wave in the visible band ( $\lambda=633$  nm). We take the gap for E7, which is the nematic liquid crystals mixture. For metal, we took a particular frequency dependence on their dielectric permittivity  $\epsilon_{Ag}(\lambda)$ . We finally find the basic characteristics for SPP. Based on the results, we have shown that the guide modes depend on its shape (dimensions). This dependence provides a means to control the propagation length, depending on the thickness.

## References

- [1] Zhanghua Han and Sergey I Bozhevolnyi. (2013). "Radiation guiding with surface plasmon polaritons," *Rep. Prog. Phys.* **76**, 016402 (37pp)
- [2] Jiri Homola. (2006). "Electromagnetic Theory of Surface Plasmons," *Springer Ser Chem Sens Biosens*, **4**: 3–44
- [3] Jun Li, Chien-Hui Wen, Sebastian Gauza, Ruibo Lu, and Shin-Tson Wu. (2005). "Refractive Indices of Liquid Crystals for Display Applications," *IEEE/OSA journal of display technology*, **1** (1), September
- [4] Jun Li, Sebastian Gauzia, and Shin-Tson Wu. (2004). "High temperature-gradient refractive index liquid crystals," **12**, (9) / *optics express* 2002-2010
- [5] Bedjaoui L, Gogibus N, Ewen B et al. (2004). Preferential salvation of the eutectic mixture of liquid crystal E7 in a polysiloxane. *Polymer*. **45**: 6555-6560
- [6] A. D. Rakic', A. B. Djuricic, J. M. Elazar and M. L. Majewski. (1998). "Optical properties of metallic films for vertical-cavity optoelectronic devices," *Applied Optics*, **37**, 22, 5271–5283
- [7] Prade, B., J. Y. Vinet and A. Mysyrowicz. (1991). "Guided waves in planar heterostructures with negative dielectric constant," *Phys. Rev. B*, **44** (24): 13556-13572
- [8] E. N. Economou. (1969). Surface plasmons in thin films" *Phys. Rev.* **182**, 539
- [9] R. Zia, M. D. Selker, P. B. Catrysse, M. L. and Brongersma. (2004). *J. Opt. Soc. Am. A*, **21**, 2442
- [10] M. A. Ordal, L. L. Long, R. J. Bell, S. E. Bell, R. R. Bell, R. W. Alexander, Jr., and C. A. Ward. (1983). Optical properties of the metals Al, Co, Cu, Au, Fe, Pb, Ni, Pd, Pt, Ag, Ti, and W in the infrared and far infrared, *Applied Optics*, **22** (7), 1099-1120
- [11] S. I. Bozhevolnyi and T. Søndergaard. (2007). General properties of slow-plasmon resonant nanostructures: nano-antennas and resonators," **15** (17), *optics express* 10869
- [12] Jiri Homola. (2008). "Surface Plasmon Resonance Sensors for Detection of Chemical and Biological Species," *Chem. Rev.* **108**, 462-493
- [13] A. Vial, A. S. Grimault, D. Macias, D. Barchiesi and M. Lamy de la Chapelle. (2005). Improved analytical fit of gold dispersion: application to the modeling of extinction spectra with a finite-difference time-domain method. *Phys. Rev. B* **71**:085416
- [14] Dionne, J. A., et al. (2006). Plasmon slot waveguides: Towards chip-scale propagation with sub wavelength-scale localization. *Phys. Rev. B* **73**(035407)

- [15] T. H. Isaac, J. Gómez Rivas, J. R. Sambles, W. L. Barnes,<sup>1</sup> and E. Hendry. (2008). "Surface plasmon mediated transmission of subwavelength slits at THz frequencies," *Phys. Rev. B*, **77**, 113411
- [16] Jianjun Chen, Zhi Li, Yujiao Zou, Zhongliang Deng, Jinghua Xiao and Qihuang Gong. (2013). "Coupled-Resonator-Induced Fano Resonances for Plasmonic Sensing with Ultra-High Figure of Merits," *Plasmonics*
- [17] Z.-D. Zhang, H.-Y. Wang and Z.-Y. Zhang. (2013). "Fano Resonance in a Gear-Shaped Nanocavity of the Metal–Insulator–Metal Waveguide," *Plasmonics* **8**:797–801
- [18] Ye Liu, Fei Zhou, Bo Yao, Jie Cao, Qinghe Mao. (2013). "High-extinction-ratio and low-insertion-loss Plasmonic Filter with Coherent Coupled Nano-cavity Array in a MIM Waveguide," *Plasmonics* **8**:1035–1041
- [19] Sonia M. García-Blanco, Markus Pollnau and Sergey I. Bozhevolnyi. (2012). "Theoretical study of loss compensation in long-range dielectric loaded surface plasmon polariton waveguides," *MINAP* (85-88)
- [20] Yao Kou and Xianfeng Chen. (2011). "Multimode interference demultiplexers and splitters in metal-insulator-metal waveguides, **19**, 07 / *optics express* (6042-6047)
- [21] Zhe Yu, Ruisheng Liang, Pixin Chen, Qiaodong Huang, Tingting Huang and Xingkai Xu. (2012). "Integrated Tunable Optofluidics Optical Filter Based on MIM Side-Coupled-Cavity Waveguide," *Plasmonics* **7**:603–607
- [22] Kunhua Wen, Lianshan Yan, Wei Pan, Bin Luo, Zhen Guo, Yinghui Guo & Xiangang Luo. (2013). "Design of Plasmonic Comb-Like Filters Using Loop-Based Resonators," *Plasmonics* **8**:1017–1022
- [23] F. I. Baida and A. Belkhir. (2012). "Finite Difference Time Domain Method for Grating Structures, *Gratings: Theory and Numeric Applications*," E. Popov (Ed.) 9.1-9.36
- [24] <http://optiwave.com>

